



## Enhancement of Thermoelectric Properties of P3HT by Addition of Carbon Nanotubes

Arif<sup>1,\*</sup>, Muhammad Tahir<sup>2</sup> and Hijaz Ahmad<sup>3</sup>

<sup>1</sup>Department of Physics, Abdul Wali Khan University (AWKUM), Mardan, Pakistan  
e-mail: arifkhanphysics1988@gmail.com

<sup>2</sup>Department of Physics, Abdul Wali Khan University (AWKUM), Mardan, Pakistan

<sup>3</sup>Department of Basic Sciences, University of Engineering and Technology Peshawar, Pakistan

\* Corresponding author

### Abstract

In this paper, the enhancement in the thermoelectric properties of the organic semiconducting material, poly(3-hexylthiophene) (P3HT) by addition of carbon nanotubes (CNTs), have been studied for applications in the renewable energy. For this purpose, the thin film of P3HT: CNTs blend has been deposited on the glass substrate by drop casting technique. The blend is prepared by the ratio of 10: 0.5 mg of P3HT: CNTs at room temperature in chloroform. The thickness of P3HT: CNTs nanocomposite found by ellipsometer was 2570 nm. The Seebeck coefficient of the film is measured to be 58.18  $\mu\text{V/K}$  and the electrical conductivity of nanocomposite was 254 S/cm found by four probe method. The bandgap of P3HT: CNTs nanocomposite was 1.4 eV measured by UV-Vis spectrometer. In this blend, the CNTs are used for enhancement of the thermoelectric properties of the film. The films are also characterized by different material characterization techniques. These characterizations are correlated with the thermoelectric properties of the material. The optimized value of the figure of merit (ZT) for the thin film has been achieved  $ZT = 0.14$  for the P3HT: CNTs nanocomposites.

Received: March 29, 2019; Accepted: May 4, 2019

Keywords and phrases: P3HT, carbon nanotubes, scanning electron microscopy, X-ray diffraction, Seebeck coefficient.

Copyright © 2019 Arif, Muhammad Tahir and Hijaz Ahmad. This is an open access article distributed under the Creative Commons Attribution License, which permits unrestricted use, distribution, and reproduction in any medium, provided the original work is properly cited.

## Introduction

Nanoscale energy is very important for mankind and its demand is growing day by day according to the lifestyle and with the increase in population. To overcome the energy needs, scientists are investigating alternate and renewable energy sources as the conventional energy sources are hazardous due to the emission of toxic gases. One of the alternate energy sources is thermoelectric energy harvesting which is based on the conversion of heat energy into electrical energy. It is favourable due to its comparatively low cost and has no hazardous environmental effect. In comparison to photovoltaic energy, it is more suitable due to easy maintenance and no moving parts. Thermoelectric properties can be observed in many materials like conductors and semiconductors.

In TE effect, an electric potential is generated in any isolated material that is subjected to a temperature gradient. The generated thermo-electric voltage is proportional to the temperature gradient checked by the equation  $dV = SdT$ , where  $S$  represents the Seebeck coefficient, named after the discoverer of the effect. Similar associated effect to Seebeck effect is Peltier effect and Thomson effect.

Mainly the efficiency of thermoelectric materials, which depends upon on the thermoelectric parameters is given by the dimensionless figure of merit,

$$ZT = S^2\sigma T/\kappa. \quad (1)$$

In the above equation,  $\sigma$  is the electrical conductivity;  $S$ ,  $T$  and  $\kappa$  are Seebeck coefficient, absolute temperature and thermal conductivity, respectively. According to (1), a good TE device should have a high electrical conductivity like that of metal, a high Seebeck coefficient like that of insulators and a low thermal conductivity like that of glass [1]. The focus of research worldwide is to enhance the figure of merit of TE devices.

For achieving the best thermoelectric properties of the thermoelectric materials (TE) and devices, two approaches are being used. One approach involves the utilization of new groups of advanced bulk thermoelectric materials and the other approach is based on using low dimensional nanostructured materials. In the first approach, heavy ion species with great vibrational amplitudes provides effective phonon-scattering centres to decrease thermal conductivity. The phonon-glass/electron-crystal is used for scattering phonon and allows conducting electron to achieve the best thermoelectric properties. In the second approach, two ideas are used. Firstly, increase the Seebeck coefficient;

introduce the nanoscale constituent in the materials which would lead to the quantum confinement effect. Quantum confinement effect enhances the power factor  $S^2\sigma$ . Secondly, nanostructure materials have many interfaces, which could increase the electrical conductivity more than the thermal conductivity and would also cause electron filtering effect to increase Seebeck coefficient [2]. Boltzmann transport equation shows the coupling of  $S$  and  $\sigma$  in such a way that increasing one would cause a decrease in another and hence it is difficult to control these two parameters independently. Similarly,  $\sigma$  and  $\kappa$  are also coupled according to Wiedemann-Franz law [3]. Decoupling among these parameters is most important for high figure of merit, which can be obtained from the heterogeneous system by mixing of two or more than two different materials, which may provide a simple way to optimize these parameters independently without affecting the others. Organic semiconducting polymers can be used in TE applications due to their low cost, easy processing, flexible nature and having low thermal conductivity. Organic semiconducting polymers can easily be mixed with other materials and make a heterogeneous system of one's own desire.

Carbon nanotubes (CNTs) are large molecules of pure carbon having diameter 1-3nm in tube-like shape. The CNTs have very strong bonding between the atoms and it also has extreme aspect ratios [4]. CNTs mainly have two types.

1. Single-walled carbon nanotubes (SWCNT)
2. Multi-walled carbon nanotubes (MWCNT)

The three dimension (3D) maps of single wall and multi-wall CNTs are given in the following Figure 1.

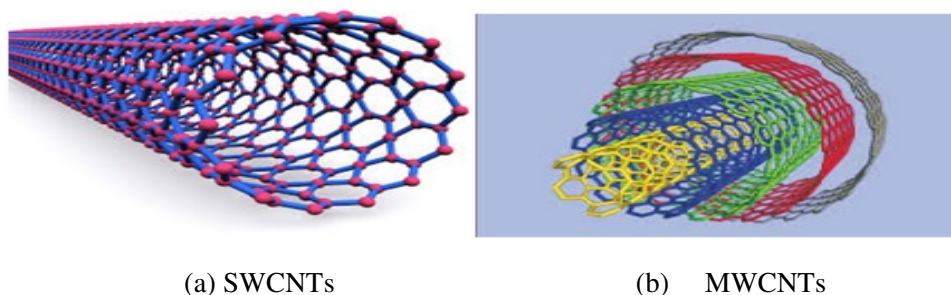


**Figure 1.** Schematic diagram of SWCNTs and MWCNTs [5].

The density of SWNT is 1.3 to 1.4 g/cm<sup>3</sup> and MWNT is 1.8 g/cm<sup>3</sup>. In CNTs length to diameter ratio =  $1.32 \times 10^8$  which is larger than all investigated materials. CNTs have high tensile strength and density, which is 100 times stronger and 6 times lighter than steel. These properties of CNTs have many potential applications in the field of organic semiconducting materials and nanoscale electronics (transistor in a single module). The issue of the transport mechanism in the organic electronic can be resolved by the incorporating of CNTs, which enhance the charge carrier mobility and provide the mechanical strength to make the polymers stable.

In this paper, we work on efficiency enhancement of TE properties of solution processable organic semiconductor P3HT by adding CNTs. First, we will achieve the optimized ratio of P3HT and CNTs to make the heterogeneous system and then will grow a thin film of the optimized blend by solution processable techniques to investigate its TE properties. Other optimum conditions of the grown film such as thickness and annealing temperature will also be achieved for detailed investigation. All these investigations will be correlated to the surface morphology and the structural analysis of the grown film.

## Characterization Techniques

There are many characterization techniques used for different purposes, i.e., scanning electron microscopy (SEM) is done for surface morphology, four probes are used to check electrical conductivity, UV-visible is used for finding bandgap and Seebeck effect is measured with the help of Seebeck set up.

### *Scanning electron microscopy (SEM)*

Surface morphology of thin film is investigated by scanning electron microscopy. The film is kept in the vacuum chamber, which is mounted on the table to avoid the vibrations. When SEM is connected to electricity, the cathode is heated up and electron gun starts ejecting electronic beam. The beams accelerated through anode plates. The accelerated beam is focused by focusing the magnetic lens towards the sample. The secondary ejected electrons from the sample are detected by the detector that shows the surface morphology of the sample on a computer screen. A high-resolution image is obtained on the computer screen by the ejection of scan dray electron from the sample surface along with the backscattered electron and characteristic X-rays. The diagram of SEM is shown in Figure 2.

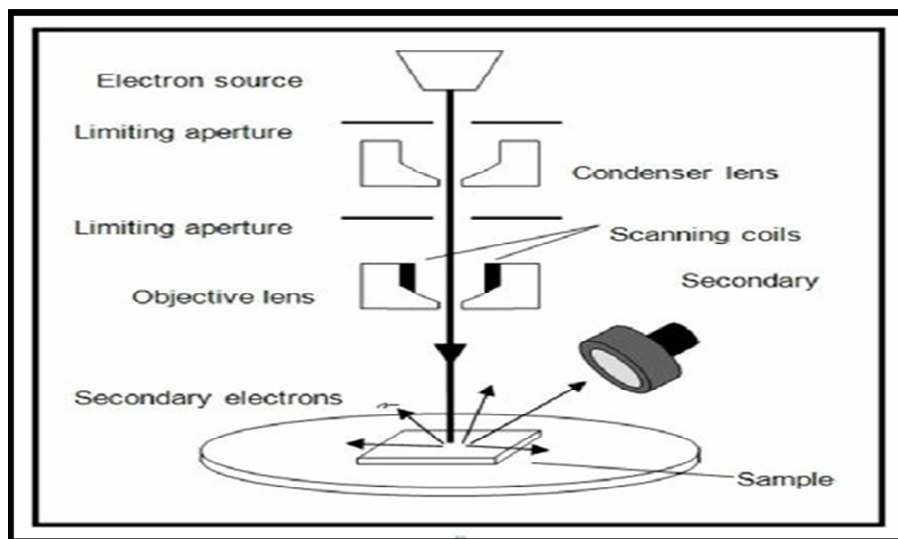


**Figure 2.** Schematic diagrams of SEM.

### *Four-point probe method*

The four-point probe is an experimental setup used for resistivity measurement of a semiconducting material through sheet resistance. Four-point probe setup is shown in Figures 3 and 4.

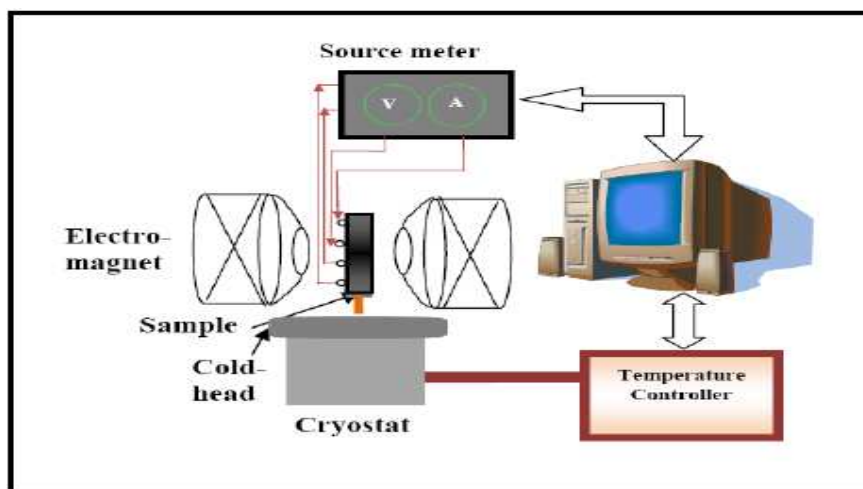


**Figure 3.** Schematic diagram of resistivity measurement.

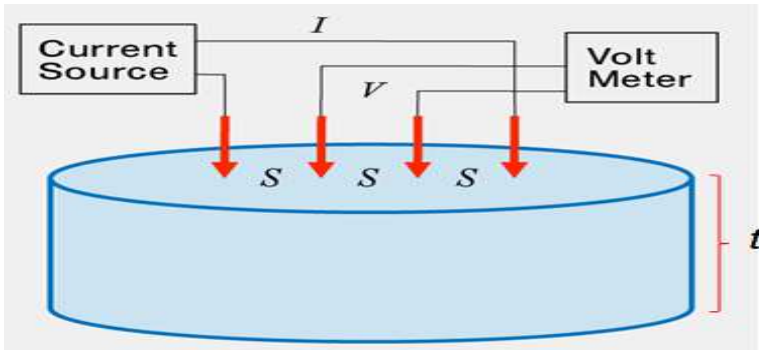


**Figure 4.** Model for the 4-point probe resistivity measurement for bulk materials.

The sheet resistance of the thin film is determined by the following formula,

$$\rho = 2\pi S(V/I). \quad (2)$$

Here  $S$  is the space between the needles, the voltage between the inner probes is represented by  $V$ , the current through the outer probe is represented by  $I$  and  $\rho$  is the resistivity of the sheet. This analysis can also be done for a rectangular sample which is shown in the Figure 5.

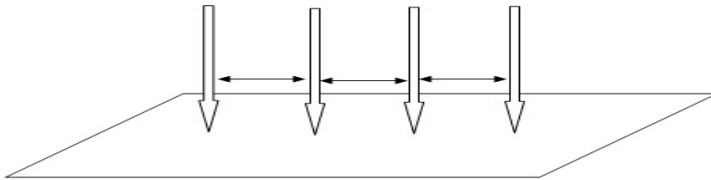


**Figure 5.** Four probe technique for rectangular sample.

The probes in the apparatus are placed at a distance  $S$  from each other and are in contact with the sample surface. The voltage is induced between the inner probes by the flow of current through the outer probes. Sheet resistance having unit  $\Omega/\text{sq}$  was calculated by using the equation:

$$\rho = \frac{V}{I}. \quad (3)$$

In the above equation,  $V$  shows the correction factor, which is different for different materials depending upon the geometry of materials. The product of sheet resistance and thickness of thin film gives the resistivity of materials. The electrical conductivity of thin film can be calculated by

$$\sigma = 1/\rho. \quad (4)$$

### Seebeck coefficient measurement setup

The thermoelectric power of materials is determined by the following equation,

$$S = \Delta V / \Delta T, \quad (5)$$

where  $\Delta V$  is the voltage build up between the hot and cold block of thermoelectric material and  $\Delta T$  is the variation in temperature between them. Seebeck set up mainly consists of a thermocouple and a voltmeter. The variation in temperature between the hot and cold side is often measured by a thermocouple while the voltage induced between them is measured by a voltmeter. The thermoelectric power of the sample is determined by suspending it between two blocks having different temperature. The experimental setup of Seebeck measurement is shown in Figure 6.

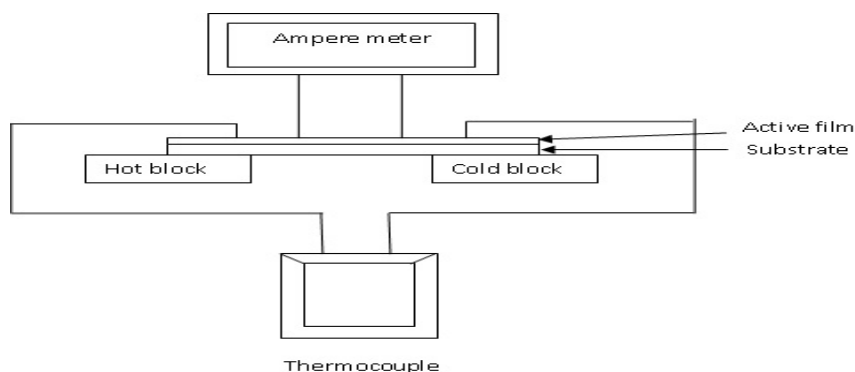


**Figure 6.** Seebeck coefficient measurement set up.

### Film deposition

The blend of the materials is formed by the combination of the poly(3-hexylthiophene) and carbon nanotubes (CNTs). Firstly, we dissolve 10 mg of P3HT in 10 ml of chloroform at room temperature. The solution is made with the help of magnetic stirrer for two hours. Now we are interested to form the blend of P3HT and CNTs with an amount of 0.5 mg. The glass substrate is rinsed with acetone for 15 minutes and then dried with the help of nitrogen gas. Finally, the thin film is deposited on a glass substrate with the help of drop casting.

### Vacuum thermal evaporator

Physical vapour deposition process used to sublime of the organic and inorganic materials for deposition purpose. It consists of the vacuum chamber which can maintain

a pressure of  $10^{-5}$ - $10^{-6}$  mbr. The vacuum chamber is used to avoid external particles contamination with vapours of sublimated particles. Evaporated material is placed boat inside the vacuum chamber and substrate is placed in the substrate holder. When the power supply is turned on, the boat in the vacuum chamber starts heating up along with the material. The material starts evaporating and spreads throughout the chamber, the particles travel toward the substrate and get deposited on the substrate surface.

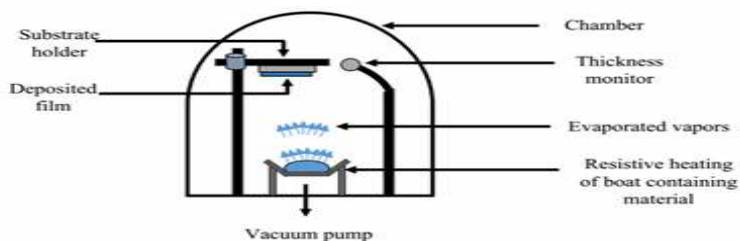


**Figure 7.** Schematic diagram.



**Figure 8.** Real picture of vacuum thermal evaporator.

This process uses a strong vacuum environment, and so is capable of producing very high purity thin films. Moreover, the deposition rate is high and damage to the substrate during deposition can be optimized. It is very simple, low-temperature process, where easily evaporated substances that easily pass into clean products are reduced, less corrosion and energy consumption is possibly less than in evaporation.

### ***X-ray diffraction technique***

The bending of a beam of radiation or particles, such as the X-ray beam, after interaction with mater, is called X-ray diffraction. X-ray diffraction (XRD) is an experimental method used to determine the crystallographic structure of a material.



Diffractometer is an instrument used for X-ray diffraction to analyze the structural information of the materials. It is easy to use the electron and neutron having a wavelength smaller than a nanometer. The electron does not penetrate deeply through the material and it gives information only about the surface of materials. While the neutron does penetrate through materials having the advantage to interact with different atoms of the materials. The X-ray diffractometer is shown in Figure 9.



**Figure 9.** Apparatus of X-ray diffraction.

X-rays are electromagnetic radiation which easily penetrates through materials and hence give the structural information such as crystallinity and phase of the materials. It is a non-destructive technique. It consists of source radiation, a monochromator for the wavelength selection, slit to regulate the shape and intensity of the beam, a sample and a detector. In additionally advanced diffractometer, a goniometer can also be used for fine adjustment of the sample and the detector position. In material science, the powder diffraction technique can be used for the structural information, while structural biological technique can be used for life sciences.

### ***Ultraviolet-visible (UV-Vis) spectroscopy***

It is a scientific technique, which produces the spectra of the investigated matter after the interaction of electromagnetic radiation with matter. The interaction occurs in the Ultraviolet-Visible (UV-Vis) range (200 nm-800 nm), the spectroscopy is called UV-Vis spectroscopy. In this spectroscopy, the light is absorbed, emitted and scattered by materials object and gives the information about the quality of the materials. In UV-Vis spectroscopy, initially, the light has the intensity  $I$  fall on the surface of the object, absorbed and becomes  $I_0$ . Transmittance is the ratio of  $I$  to  $I_0$ , i.e.,  $I/I_0$ . The transmission spectrum gives the optical band gap as given by Tauc's law:

$$\alpha E = (E - E_g)^m. \quad (6)$$

Here  $\alpha$  is the absorption coefficient and can be calculated as

$$T = \frac{I}{I_0} = \exp(-\alpha d) \quad (7)$$

$$-\ln T = \alpha d. \quad (8)$$

In the equation (7),  $d$  represents the film thickness.

### **P3HT: CNTs Thin Film (Blend) Characterization**

Morphological investigation of the thin film (blend) is very important for thermoelectric application and electrical conductivity. It gives information about roughness, the orientation of atoms in the blend and different peaks. In morphology, we are interested to study interfaces between the grains or interfaces are investigated for better performance of materials for their potential thermoelectric applications. Usually, thermal and electrical conductivities are coupled with each other in every material, so incorporation of carbon nanotubes decoupled these parameters to some extent to achieve better performance rather than pure P3HT and CNTs separately. The band gap is found by spectroscopic technique, which plays an important role in the performance of the thin blend. Small band gap materials have high performance than the large band gap materials.

#### ***Morphology of P3HT: CNTs***

There are many techniques used to investigate surface morphology of the materials such as scanning electron microscopy (SEM), atomic force microscopy (AFM), scanning probe microscopy (SPM) and field emission scanning electron microscopy (FESEM) etc. The usage of each technique depends upon the surface nature and availability of the instrument. We have used SEM in our research.

#### ***Scanning electron microscopy***

Figure 10 shows the SEM image of P3HT: CNTs nanocomposite to study its surface morphology. The image reveals agglomeration of CNTs in the matrix of P3HT. A high-resolution image is depicted with 5000 magnifications by applying 10 kV accelerating voltage. The pure P3HT and SWCNTSSEM image are shown the following figures (a) P3HT [6] and (b) SWCNTs [7].

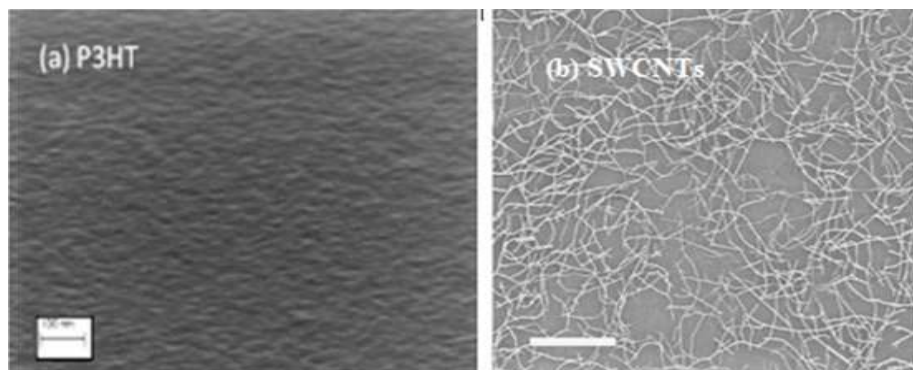


**Figure 10.** SEM image of pure P3HT and CNTs[6].

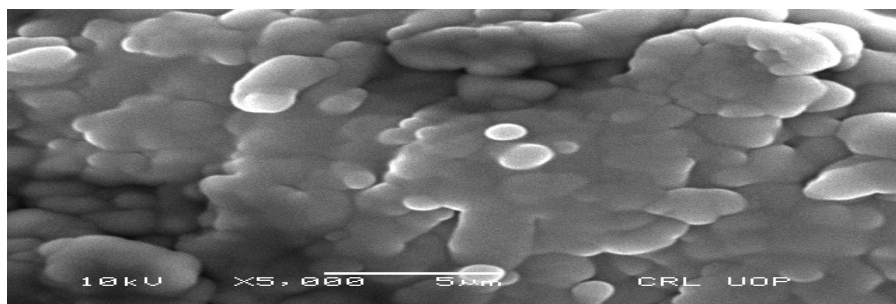


**Figure 11.** SEM image of P3HT: CNTs blend with 5 μm scale.

The amorphous structure of P3HT enhances the Seebeck coefficient of the device. While the CNTs increasing the electrical conductivity without increasing thermal conductivity. CNTS provides a barrier (interfaces) which improve the scattering of phonons and filtering electrons respectively.

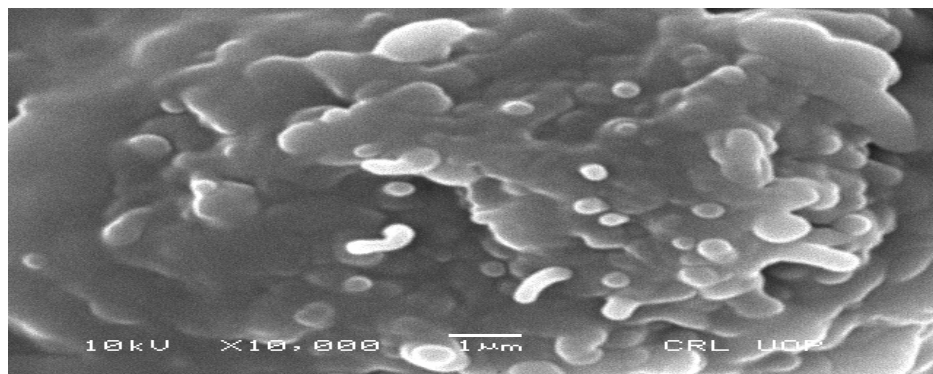


**Figure 12.** SEM image of P3HT: CNTs blend with 1 μm scale.

The surface of the blend is different from the surfaces of independent P3HT and CNTs. This discrimination is due to the mixing of CNTs with a specific ratio of P3HT.

### UV-Vis spectrum of P3HT: CNTs

The bandgap plays an important role in the efficiency of the semiconducting materials. In this research work, the addition of CNTs in the P3HT matrix, the absorption spectrum of pure P3HT is shifted from the visible region 500 nm to the ultraviolet region 281nm. The electrical conductivity of P3HT in the neutral state is very low in electrochemical measurement as considered to be non-conducting semiconductor polymer, but by doping it becomes conducting polymer [7].

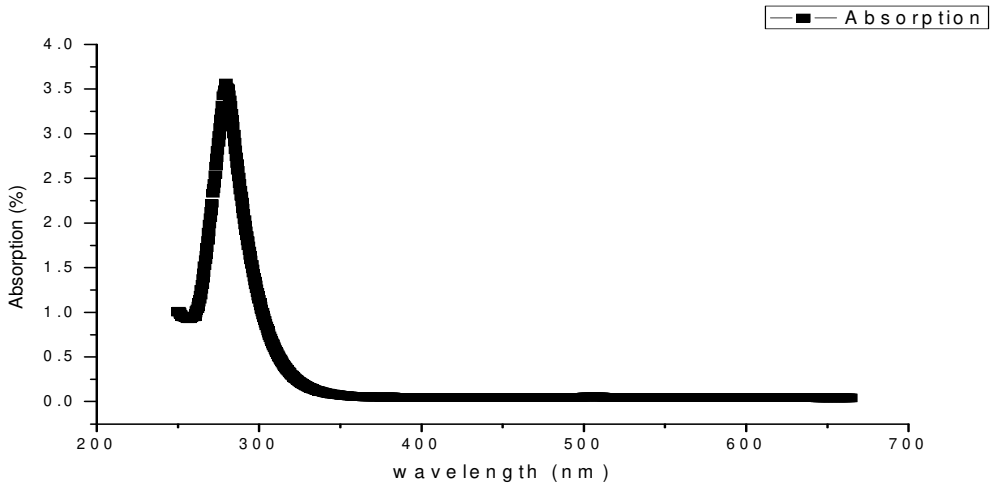


**Figure 13.** UV-Vis spectrum of P3HT: CNTs blend.

To calculate the bandgap, the Tauc's law is applied, i.e.,

$$\alpha E = (E - E_g)^m. \quad (9)$$

In this equation, the absorption coefficient is represented by  $\alpha$  which is given as:

$$A = -\ln\left[\frac{I}{I_0}\right] \Rightarrow A = \alpha d. \quad (10)$$

In this equation,  $E$  is the photon energy,  $E_g$  is the band gap energy,  $d$  shows the film thickness and  $m$  is the transition constant. Furthermore,  $m$  takes the value of "2" for indirect transition and of  $\frac{1}{2}$  for the direct transition.

Our material is direct bandgap semiconductor, so we have used direct transition model. For the P3HT: CNTs blend the calculated energy band gap is about 1.4 eV, while the reported one is 1.9-2 eV [8]. In the figure below the  $(\alpha E)^2$  and  $E$  is plotted as:

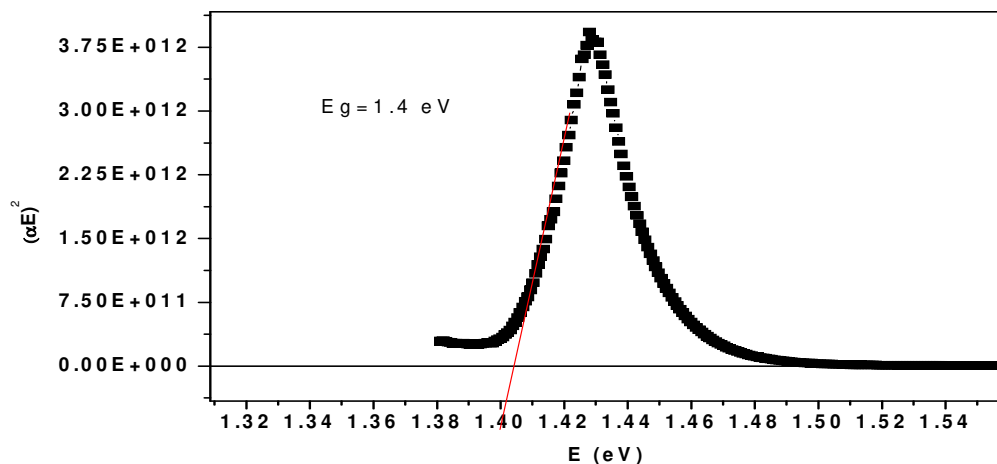


**Figure 14.** Band gap measurement of P3HT: CNTs blend.

### *X-ray diffraction (XRD)*

To investigate the nature of the film, diffractogram of the blended thin film made from the combination of P3HT and CNTs is obtained by X-ray diffraction method. The structure P3HT is not affected by incorporation of CNTs in the blend for a range of 15 to 20 degree [9]. There are some portions of the spectrum represents the amorphous structure and some peaks represent the crystalline nature due to the nanocomposite structure of blend. At room temperature, the P3HT has purely amorphous nature. While the annealed P3HT has some order of crystalline nature. There are only two prominent peaks occur due to the inclusion of CNTs, which are located at the positions, 37 and 45 degree respectively compared with that of reported in the literature [10].

The power factor of P3HT: CNTs blend have improved value due to the amorphous nature of P3HT and crystalline nature of CNTs. The images of pure P3HT: CNTs and P3HT: CNTs blend are shown in Figures 15 and 16 [11, 12].

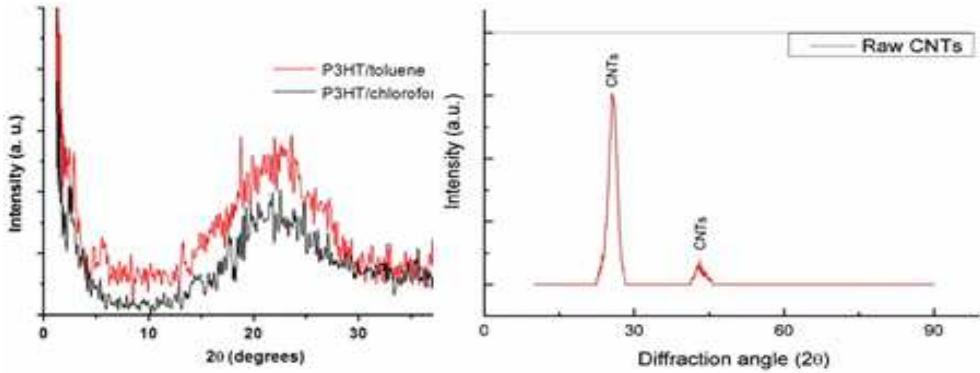


**Figure 15.** XRD image of pure P3HT and CNTs [11].

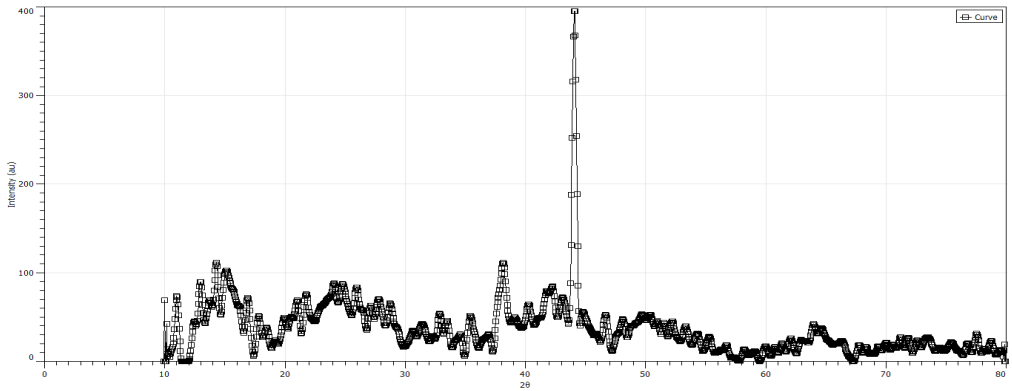


**Figure 16.** XRD image of P3HT: CNTs blend.

## Electrical Conductivity of the Material

The four-point probe method is used to measure the value of the electrical conductivity of the P3HT: CNTs film. The current is passing through the outer probes which induced the emf between the inner probes.

In this research work, the value for electrical conductivity is measured to be 254 S/cm of the P3HT: CNTs blend is obtained, which is very high as compared to the pure P3HT electrical conductivity  $10^{-4}$ - $10^{-5}$  S/cm.

### *Seebeck coefficient measurement*

The Seebeck coefficient or thermoelectric power of the sample was calculated by holding the sample between two blocks controlled by temperature. One end of the

thermocouple is kept at high temperature and the other at a low temperature. The thermal voltage can be induced in it measured by micro voltmeter.

The graph for Seebeck coefficient of P3HT: CNTs blend is given in Figure 17.

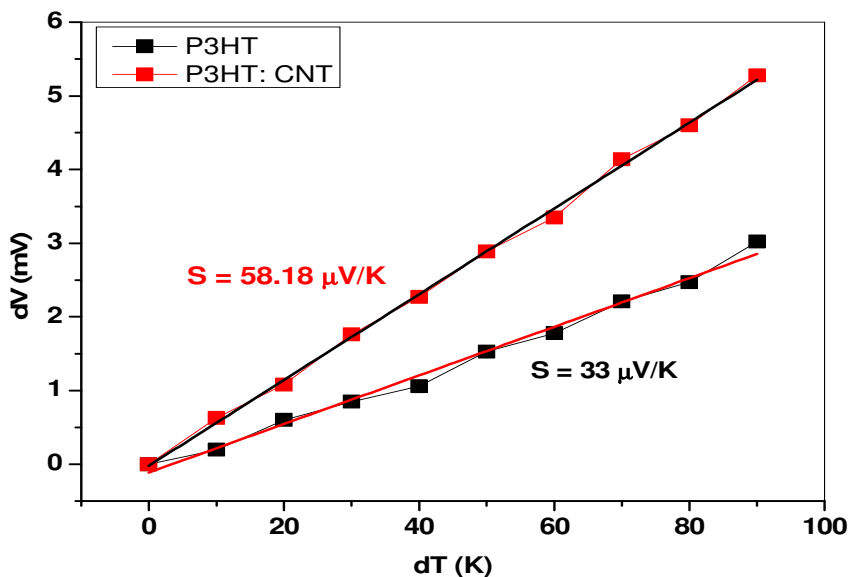


**Figure 17.** The graphs of Seebeck coefficient for pure and P3HT: CNTs blend.

The measured thermal voltage varied linearly with the increase in temperature. The value of the Seebeck coefficient for pure P3HT is  $33\mu\text{V/K}$ . While the obtained value for the P3HT: CNTs blend is  $58.18\mu\text{V/K}$ .

Mathematical formula of Seebeck coefficient is given below.

$$S = \Delta V / \Delta T . \quad (11)$$

In the above equation,  $S$  represents Seebeck coefficient,  $\Delta V$  is the thermal voltage between the two ends of the sample and  $\Delta T$  is a temperature difference of ends sample holder. The graph shows p-type nature of the material.

### Figure of Merit (ZT) of Ag/ P3HT: CNTs/Ag

The numerical quantity used to check the performance of the thermoelectric device is called a figure of merit. It depends upon Seebeck coefficient or thermo-power, electrical conductivity and thermal conductivity of the device. The figure of merit can be

correlated by the quantities, which are given as,

$$ZT = \frac{S^2 \sigma}{\kappa} T. \quad (12)$$

Mathematically the thermal conductivity is defined as,

$$\kappa = \kappa_l + \kappa_e. \quad (13)$$

Here  $\kappa_e$  is the contribution of electrons or holes and  $\kappa_l$  is the lattice (phonon's) contribution. By making a blended film, the phonon contribution minimized thermal conductivity significantly and hence major contribution is due to electronic thermal conductivity. The electronic thermal conductivity of the film was estimated from the following relation:

$$\kappa_e = \sigma LT. \quad (14)$$

Lorentz factor is represented by  $L$  and its value for free electrons is to  $2.4 \times 10^{-8} \text{ J}^2 \text{ K}^{-2} \text{ C}^{-2}$  [13] and  $T$  in our case is room temperature. The electrical and thermal conductivities for pure P3HT are  $10^{-4}$ - $10^{-5} \text{ S/cm}$  and  $0.7 \text{ nW/K.cm}$  respectively, while for the blend of P3HT: CNTs are  $254 \text{ S/cm}$  and  $1.82 \text{ mW/K.cm}$ .

In this research work we obtained the figure of merit ( $ZT$ ) of pure P3HT as 0.003 and for the blend of P3HT: CNTs as 0.14. Blended film result is about 1000 times better than the pure P3HT film.

Low thermal conductivity and high electrical conductivity are good for thermoelectric materials, but this is impossible for inhomogeneous materials. Increase in electrical conductivity by increasing the concentration of charges in the materials unavoidably increases thermal conductivity. Researchers have tried to decouple these two quantities. Nano-engineering provides the pathway to decouple these two quantities in the homogeneous materials by introducing interfaces. An interface reduces thermal conductivity at the boundary without affecting the electrical conductivity.

The below table presents present research with the other organic materials [14].



**Table 1.** Seebeck coefficient and figure of merit of current research work with past.

Matrix	Dopant	Electrical conductivity (s/cm)	Seebeck Coefficient ( $\mu\text{v/K}$ )	Power factor ( $\mu\text{WmK}^{-2}$ )	ZT evaluated
P3HT <sup>1</sup>	F <sub>4</sub> -TCNQ	$3.8 \times 10^{-4}$	400	0.006	$0.8 \sim 1.1 \times 10^{-6}$
P3HT <sup>2</sup>	NOPF <sub>6</sub>	2.2	25	0.14	$1.9 \sim 2.5 \times 10^{-4}$
P3HT <sup>3</sup>	FeCl <sub>3</sub>	7	74	3.9	$5.3 \sim 7.1 \times 10^{-3}$
P3HT <sup>4</sup>	FeCl <sub>3</sub> NOPF <sub>6</sub>	21	30	1.9	$2.6 \sim 3.4 \times 10^{-3}$
P3HT <sup>5</sup>	Fe(TFSI) <sub>3</sub>	10	36	1.3	$1.8 \sim 2.4 \times 10^{-3}$
P3HT <sup>6</sup>	CNTS	91	49	21.8	0.03 ~ 0.04
P3HT	pure	254	58.18		0.14
P3HT		$10^{-4} \sim 10^{-5}$	33		$3 \times 10^{-3}$

## Conclusion

In this paper, the thermoelectric properties and Seebeck coefficient of Ag/P3HT: CNTs/Ag device has been significantly improved by developing P3HT-CNTs nanocomposite film. The thickness of the drop cast film of P3HT: CNTs nanocomposites was 2570 nm which was measured by an ellipsometer. The electrical conductivity of P3HT has been greatly enhanced from  $10^{-4}$  S/cm to 254 S/cm by adding CNTs. However, the thermal conductivity of pure P3HT and P3HT: CNTs nanocomposites were measured to be 0.7 nW/K.cm and 1.82 mW/K.cm, respectively. Hence, for the Ag/P3HT/Ag thermoelectric device figure of merit ZT was 0.003 while for the Ag/P3HT: CNTs/Ag device it was found to be 0.140. Conclusively, this enhancement in ZT is attributed to the enormous increase in electrical conductivity of P3HT: CNTs nanocomposites. Moreover, XRD of the nanocomposite film revealed amorphous nature. The morphological study by SEM of the composited film has a magnification of 5000 and grain size of 5 microns at 10 kV accelerating voltage. The bandgap of the composite film was 1.4eV from the UV-Vis spectrum.

## References

- [1] G. S. Nolas, D. T. Morelli and T. M. Tritt, SKUTTERUDITES: A phonon-glass-electron

- crystal approach to advanced thermoelectric energy conversion applications, *Annual Review of Materials Science* 29 (1999), 89-116.  
<https://doi.org/10.1146/annurev.matsci.29.1.89>
- [2] M. S. Dresselhaus et al., New directions for low-dimensional thermoelectric materials, *Advanced Materials* 19 (2007), 1043-1053. <https://doi.org/10.1002/adma.200600527>
- [3] J. P. Heremans et al., Enhancement of thermoelectric efficiency in PbTe by distortion of the electronic density of states, *Science* 321 (2008), 554-557.  
<https://doi.org/10.1126/science.1159725>
- [4] N. Bhalerao, *Polypyrrole Nanocomposites Reinforced with Multi-Walled Carbon Nanotubes*, Lamar University-Beaumont, 2016.
- [5] Ahmad Aqel, Kholoud M.M. Abou El-Nour, Reda A.A. Ammar and Abdulrahman Al-Warthan, Carbon nanotubes, science and technology part (I) structure, synthesis and characterisation. *Arabian Journal of Chemistry* 5 (2012), 1-23.  
<https://doi.org/10.1016/j.arabjc.2010.08.022>
- [6] F. Zhang, Peng-Xiang Hou, Chang Liu, Bing-Wei Wang, Hua Jiang, Mao-Lin Chen, Dong-Ming Sun et al., Growth of semiconducting single-wall carbon nanotubes with a narrow band-gap distribution, *Nature Communications* 7 (2016), Art. No. 11160.  
<https://doi.org/10.1038/ncomms11563>
- [7] S. Ludwigs, *P3HT Revisited-From Molecular Scale to Solar Cell Devices*, Springer, 2014. <https://doi.org/10.1007/978-3-662-45145-8>
- [8] V. Shrotriya, J. Ouyang, R. J. Tseng, G. Li and Y. Yang, Absorption spectra modification in poly(3-hexylthiophene):methanofullerene blend thin films, *Chemical Physics Letters* 411 (2005), 138-143. <https://doi.org/10.1016/j.cplett.2005.06.027>
- [9] G. Paternó, F. Cacialli and V. García-Sakai, Structural and dynamical characterization of P3HT/PCBM blends, *Chemical Physics* 427 (2013), 142-146.  
<https://doi.org/10.1016/j.chemphys.2013.10.006>
- [10] Y. Wang, Y. Yang, X. Zhang, C. Liu and X. Hao, One-step electrodeposition of polyaniline/nickel hexacyanoferrate/sulfonated carbon nanotubes interconnected composite films for supercapacitor, *Journal of Solid State Electrochemistry* 19 (2015), 3157-3168. <https://doi.org/10.1007/s10008-015-2934-4>
- [11] L. Pan and Z. Sun, Solvent and temperature-dependent conductive behaviour of poly(3-hexylthiophene), *Journal of Physics and Chemistry of Solids* 70 (2009), 1113-1116.  
<https://doi.org/10.1016/j.jpics.2009.06.008>

- 
- [12] Ihsanullah, A. M. Al Amer, Tahar Laoui, Aamir Abbas, Nasser Al-Aqeeli, Faheemuddin Patel, Marwan Khraisheh, Muataz Ali Atieh and Nidal Hilal, Fabrication and antifouling behaviour of a carbon nanotube membrane, *Materials & Design* 89 (2016), 549-558. <https://doi.org/10.1016/j.matdes.2015.10.018>
- [13] G. J. Snyder and E. S. Toberer, Complex thermoelectric materials, *Nature Materials* 7 (2008), 105-114. <https://doi.org/10.1038/nmat2090>
- [14] S. Qu et al., Highly anisotropic P3HT films with enhanced thermoelectric performance via organic small molecule epitaxy, *NPG Asia Materials* 8 (2016), e292. <https://doi.org/10.1038/am.2016.97>